Inorganic Chemistry

Article

pubs.acs.org/IC

Ring-Shaped Rhenium(I) Multinuclear Complexes: Improved Synthesis and Photoinduced Multielectron Accumulation

Tsuyoshi Asatani,[†] Yuki Nakagawa,[†] Yusuke Funada,[†] Shuhei Sawa,[†] Hiroyuki Takeda,[†,§] Tatsuki Morimoto,[†,§] Kazuhide Koike,[†,‡,§] and Osamu Ishitani*[,†,§]

[†]Department of Chemistry, Graduate School of Science and Engineering, Tokyo Institute of Technology, 2-12-1-NE-1 O-okayama, Meguro-ku, Tokyo 152-8550, Japan

[‡]National Institute of Advanced Industrial Science and Technology, 16-1 Onogawa, Tsukuba 305-8569, Japan

[§]CREST, Japan Science and Technology Agency, 4-1-8 Honcho, Kawaguchi-shi, Saitama 322-0012, Japan

Supporting Information

ABSTRACT: We successfully developed selective synthesis of strongly emissive ring-shaped Re(I) multinuclear complexes (**RnP(*x*)**$^{n+}$ in Chart 1) with much higher yields compared with the previously reported method. This improved method could also be employed to prepare a novel ring-shaped multinuclear complex composed of structurally different Re(I) units. Each Re unit in **RnP(*x*)**$^{n+}$ could electrochemically accept one electron, and the multielectron reduced states of **RnP(*x*)**$^{n+}$ were stable. In the presence of triethanolamine, the ring-shaped tetranuclear and hexanuclear complexes can be photochemically reduced and accumulate 2.9−3.6 and 4.4 electrons in one molecule, respectively.

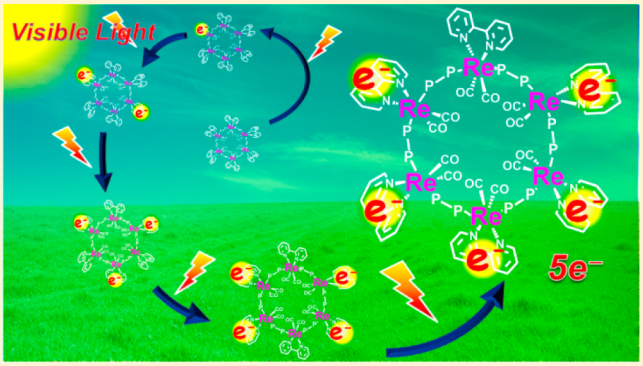

INTRODUCTION

Recently, much attention has been directed toward conversion of solar energy to storable chemical energy to mitigate global warming and shortage of energy resources. For example, photocatalysts for hydrogen evolution from water and CO_2 reduction have been extensively investigated. These photochemical reactions require multiple electrons to reduce the substrates and yield useful and stable products. Transition metal complexes, involving Ru(II),[1] Re(I),[2] Os(II),[3] and Ir(III),[4] have been often used as redox photosensitizers owing to their long lifetime and the high redox power of their excited states. However, they have an inherent limitation of a single photon absorption event inducing only one electron transfer. Thus, for conversion of solar energy to chemical energy, developing photochemical multielectron accumulation systems is important.

Some studies have been conducted regarding homogeneous systems that include a transition metal complex for photochemical multielectron storage. MacDonnell et al. reported that Ru(II) binuclear complexes with a bridging ligand, which had a tetraazatetrapyridopentacene or tetraazatetrapyridoquinone group, could accumulate two or four electrons in one molecule in the presence of an electron donor by visible light irradiation.[5a−5c] Tanaka et al. reported Ru(II) complexes with pyridylbenzonaphthyridine ligands, which photochemically accumulated six electrons in one molecule via proton-coupled electron transfer.[5d−f] Although these complexes can accumulate multiple photoinduced electrons in a single molecule, the reduction potentials are lower than that required to be useful in photocatalytic reactions, such as CO_2 reduction. Sakai et al.

Chart 1. Structures and Abbreviations of the Ring and Linear-Shaped Re(I) Multinuclear Complexes and the Corresponding Mononuclear Complex

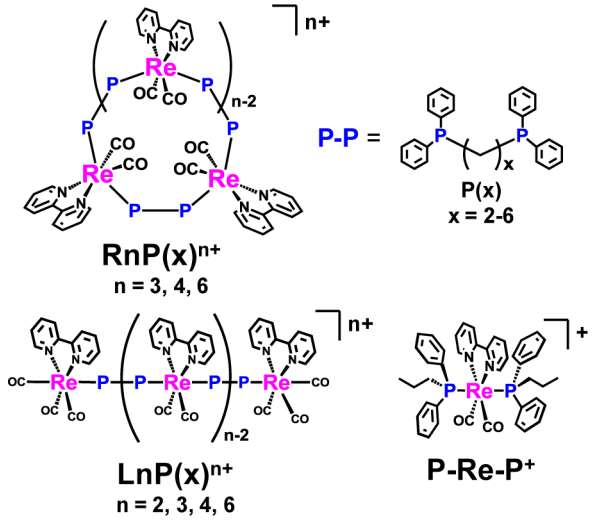

Received: January 28, 2014
Published: July 9, 2014

   dx.doi.org/10.1021/ic501196q | *Inorg. Chem.* 2014, 53, 7170−7180

recently reported that a Pt complex with four viologen-type electron acceptors could photochemically accumulate ~1.6 electrons in one molecule on an average, and excitation of the reduced complex induced H_2 evolution.[6]

We have previously reported the synthesis and photophysical properties of ring-shaped Re(I) multinuclear complexes (**RnP(*x*)**$^{n+}$ in Chart 1), comprising various numbers of repeated rhenium(I) diimine biscarbonyl bisphosphine complex units of which one-electron-reduced species (OERS) are stable and demonstrate high reduction power.[7] A series of the complexes is more efficient as a photosensitizer than the corresponding mononuclear complex because the ring-shaped multinuclear complexes have specific photophysical properties caused by strengthened $\pi-\pi$ interaction between the diimine ligands and the phenyl groups of the phosphine ligands[8] due to the rigidity of the molecular structures. When a ring-shaped Re(I) trinuclear complex with strong $\pi-\pi$ interactions was used as a photosensitizer and $[Re(bpy)(CO)_3(MeCN)]^+$ (bpy = 2,2′-bipyridine) was used as a catalyst, CO_2 was selectively reduced to CO with an 82% quantum yield.[7b]

While these complexes are promising photosensitizers, their synthesis suffers from three drawbacks. For the synthesis of the ring-shaped multinuclear complexes (eq 1), photochemical

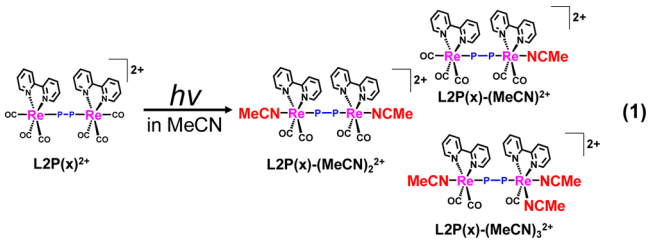

(1)

substitution of the two carbonyl ligands at trans positions to the phosphorus ligand (*trans*-**CO**) in the linear-shaped Re(I) binuclear complex (**L2P(*x*)**$^{2+}$) by MeCN solvent molecules is an important reaction.[9] Although both of the two *trans*-**CO**s of **L2P(*x*)**$^{2+}$ must be selectively substituted, mono- and trisubstituted byproducts (**L2P(*x*)-(MeCN)**$^{2+}$ and **L2P(*x*)-(MeCN)**$_3^{2+}$) are also formed because these byproducts have polarities and sizes similar to **L2P(*x*)-(MeCN)**$_2^{2+}$. The low isolated yield of **L2P(*x*)-(MeCN)**$_2^{2+}$ was one of the main reasons for the low yield of the target complex. The cyclization process of **L2P(*x*)-(MeCN)**$_2^{2+}$ afforded a mixture of not only various ring-shaped but also linear-shaped Re(I) oligomers and polymers; moreover, the difficult separation procedures also lowered the isolated yield of the target complex. In addition, previously reported methods can give rise to ring-shaped multinuclear Re(I) complexes comprised only of the same Re unit. In other words, a ring-shaped multinuclear Re(I) complex constructed with different Re(I) units has not yet been reported.

Here we report a new high-yielding targeted synthesis of ring-shaped multinuclear complexes composed of a fixed number of Re(I) units or composed of different Re(I) units. The high yields of the ring-shaped multinuclear complexes facilitate investigations into various properties and reactivities of these complexes. Consequently, the redox behavior of these complexes is reported here for the first time. Moreover, we report that the ring-shaped multinuclear complexes can accumulate many electrons in one molecule by light irradiation in the presence of triethanolamine (TEOA) as an electron donor.

RESULTS AND DISCUSSION

Photochemical Ligand Substitution Reaction. Various reaction conditions were examined for inducing selective photochemical ligand substitution of two *trans*-**CO**s in the linear-shaped Re(I) binuclear complexes. As a typical example, the photochemical reaction of **L2P(4)**$^{2+}$ is discussed. In the previously reported method using MeCN as the solvent,[7b] only one of the *trans*-**CO**s was substituted by the solvent molecule (**Sol**) for short-period photoirradiation, primarily yielding **L2P(4)-(MeCN)**$^{2+}$ (eq 2).

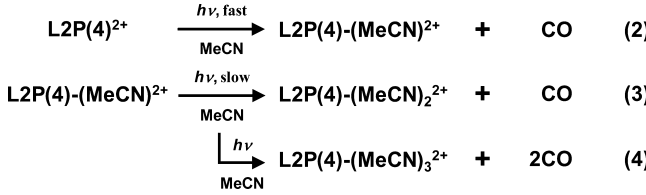

The photochemical ligand substitution reaction rate of **L2P(4)-(MeCN)**$^{2+}$ yielding **L2P(4)-(MeCN)**$_2^{2+}$ (eq 3), of which both *trans*-**CO**s were substituted with MeCN molecules, drastically decreased because of a competing energy transfer reaction from another Re tricarbonyl unit to the produced Re biscarbonyl unit in **L2P(4)-(MeCN)**$^{2+}$. Figure 1a shows the

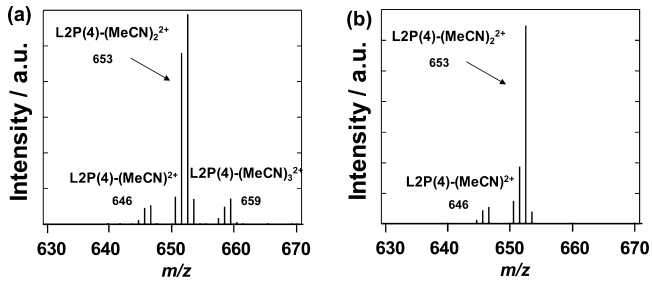

Figure 1. ESI-MS spectra acquired after irradiating (>330 nm at 25 °C) **L2P(4)**$^{2+}$ in (a) MeCN for 2 h and (b) acetone–H_2O (7:1 v/v) for 4.5 h. The eluent was MeCN.

electrospray ionization-mass spectroscopy (ESI-MS) spectrum of the reaction solution after 2 h of irradiation. The figure clearly indicates that further ligand substitution reaction of **L2P(4)-(MeCN)**$_2^{2+}$, which is the target complex in this process, also proceeded to afford **L2P(4)-(MeCN)**$_3^{2+}$, where one of the Re units had only one carbonyl ligand (eq 4), even while **L2P(4)-(MeCN)**$^{2+}$ still remained in the solution. The separation of **L2P(4)-(MeCN)**$_3^{2+}$ from **L2P(4)-(MeCN)**$_2^{2+}$ was necessary, and this procedure lowered the isolated yield of **L2P(4)-(MeCN)**$_2^{2+}$. Therefore, for suppressing **L2P(4)-(MeCN)**$_3^{2+}$ formation, various reaction conditions were examined for the photochemical ligand substitution reaction, and an acetone and water (7:1 v/v) mixture was determined to be useful for selective production of **L2P(4)-(Sol)**$_2^{2+}$ without **L2P(4)-(Sol)**$_3^{2+}$ formation (eqs 5–7, Figure 1b). **L2P(4)-(Sol)**$_2^{2+}$ was quantitatively converted to **L2P(4)-(MeCN)**$_2^{2+}$ by simple addition of MeCN into the reaction solution (eq 8). In this case, the isolation procedure was not necessary. Similarly, the photochemical ligand substitution reaction for other linear-shaped binuclear complexes selectively proceeded, and **L2P(*x*)-(MeCN)**$_2^{2+}$ could be obtained without any isolation procedures. Moreover, we determined that the photochemical ligand substitution reaction could be applied

dx.doi.org/10.1021/ic501196q | Inorg. Chem. 2014, 53, 7170–7180

$$\mathbf{L2P(4)}^{2+} \xrightarrow[\text{Acetone-Water}]{h\nu} \mathbf{L2P(4)\text{-}(Sol)}^{2+} + CO \quad (5)$$

$$\mathbf{L2P(4)\text{-}(Sol)}^{2+} \xrightarrow[\text{Acetone-Water}]{h\nu} \mathbf{L2P(4)\text{-}(Sol)_2}^{2+} + CO \quad (6)$$

$$\not\xrightarrow{h\nu} \mathbf{L2P(4)\text{-}(Sol)_3}^{2+} + 2CO \quad (7)$$

$$\mathbf{L2P(4)\text{-}(Sol)_2}^{2+} \xrightarrow[\text{MeCN}]{} \mathbf{L2P(4)\text{-}(MeCN)_2}^{2+} + 2Sol \quad (8)$$

to not only binuclear complexes but also to other multinuclear complexes, as described below.

Targeted High-Yielding Synthesis of Ring-Shaped Multinuclear Complex. In the previously reported method, the isolated $\mathbf{L2P}(x)\text{-}(\mathbf{MeCN})_2^{2+}$ was used as a starting complex for synthesis of the ring-shaped multinuclear complexes.[10] This method afforded a diverse mixture of complexes, including various linear- and ring-shaped multinuclear complexes (Supporting Information, Figure S1). Therefore, we attempted to develop selective synthesis of ring-shaped multinuclear complexes with the target number of Re units using the corresponding linear-shaped complexes with the same number of Re units.

Scheme 1 illustrates the synthesis of $\mathbf{R4P(4)}^{4+}$ as a typical example. The corresponding linear-shaped tetranuclear complex, $\mathbf{L4P(4)}^{4+}$, was synthesized in a good yield by the reported method.[10] $\mathbf{L4P(4)}^{4+}$ was irradiated in a mixture of acetone–water (7:1 v/v), which selectively yielded $\mathbf{L4P(4)\text{-}(Sol)_2}^{4+}$ (Supporting Information, Figure S2a), which was quantitatively converted to $\mathbf{L4P(4)\text{-}(MeCN)_2}^{4+}$ by the similar method described above.[11] $\mathbf{L4P(4)\text{-}(MeCN)_2}^{4+}$ was directly used in the next step without being isolated. Thermal reaction of $\mathbf{L4P(4)\text{-}(MeCN)_2}^{4+}$ with an equivalent amount of **P(4)** yielded $\mathbf{R4P(4)}^{4+}$. The overall yield based on the $\mathbf{L2P(4)}^{2+}$ used in the procedure was 38%, which was about 3 times higher than the previously reported method using $\mathbf{L2P(4)\text{-}(MeCN)_2}^{2+}$.[7b] Since $\mathbf{R4P(4)}^{4+}$ was selectively formed, purification by recrystallization was significantly more efficient than size-exclusion chromatography (Supporting Information, Figure S2b). Other ring-shaped tetranuclear complexes with various bidentate phosphorus ligands could also be obtained by a similar method, and in most cases (except for $\mathbf{R4P(5)}^{4+}$), recrystallization alone afforded the pure compound without the need for any inconvenient chromatographic methods (Table 1).

Table 1. Isolated Yields of Various Complexes by the New Method and the Previously Reported Method[a]

complex	new method [%]	previous method [%]
$\mathbf{R4P(2)}^{4+}$	40	3
$\mathbf{R4P(3)}^{4+}$	20	4
$\mathbf{R4P(4)}^{4+}$	38	10
$\mathbf{R4P(5)}^{4+}$	24	<1
$\mathbf{R4P(6)}^{4+}$	40	3
$\mathbf{R3P(2)}^{3+}$	34	8
$\mathbf{R6P(4)}^{6+}$	9	4
$\mathbf{R3P(2)(dmb_2,bpy)}^{3+}$	17	*b*

[a]Total yield based on the corresponding linear-shaped Re(I) binuclear complexes used. [b]No report.

The total yields obtained by this method were up to 24 times higher than the previously reported method. Trinuclear and hexanuclear ring-shaped complexes ($\mathbf{R3P(2)}^{3+}$, $\mathbf{R6P(4)}^{6+}$) could also be synthesized using the corresponding linear-shaped multinuclear complexes in better yields (Table 1). This targeted synthesis afforded sufficient amounts of ring-shaped multinuclear complexes, thereby allowing for the characterization of their properties and evaluation of their reactivity (see below).

Synthesis of Ring-Shaped Trinuclear Re(I) Complex Containing Different Re(I) Units. The selective photochemical reaction can be also applied to synthesis of ring-

Scheme 1. An Illustration of New Synthetic Procedure for $\mathbf{R4P(4)}^{4+}$[a]

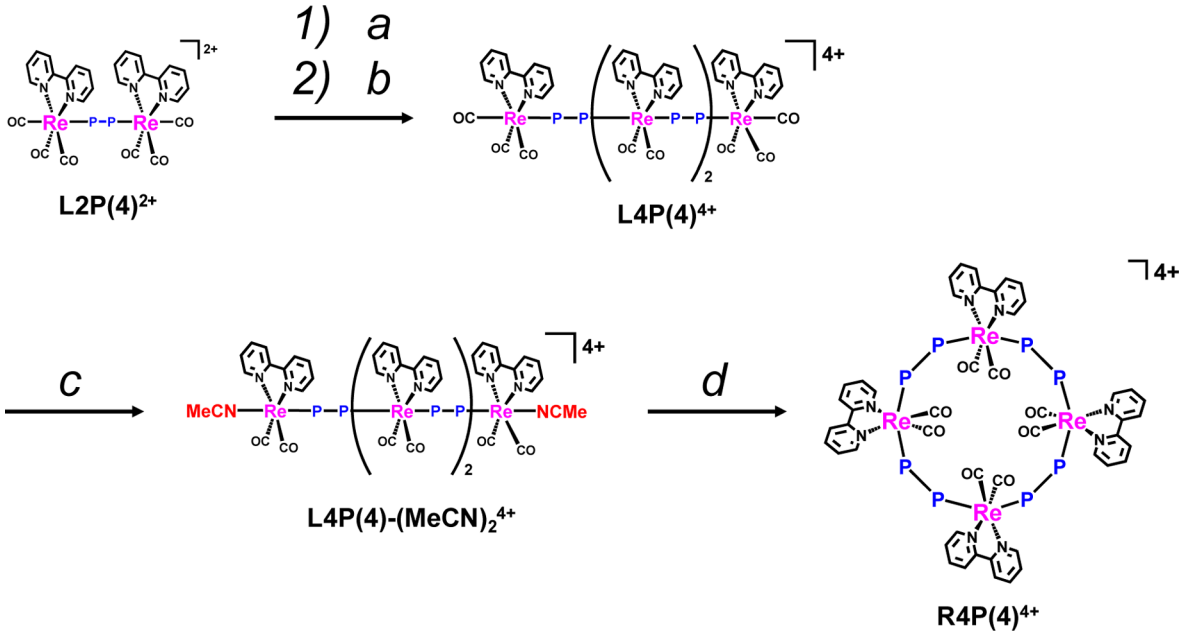

[a](a) *hν* (> 330 nm) in CH_2Cl_2 for 30 min; (b) **P(4)** (0.5 equiv), reflux in tetrahydrofuran (THF) for 2 d, then addition of MeOH containing NH_4PF_6; (c) *hν* (> 330 nm) in acetone–H_2O (7:1 v/v) for 2.5 h, and then addition of MeCN; and (d) **P(4)** (1.1 equiv), reflux in acetone for 12 h.

dx.doi.org/10.1021/ic501196q | Inorg. Chem. 2014, 53, 7170–7180

Scheme 2. An Illustration of the Procedure for Synthesis of R3P(2)(dmb$_2$,bpy)$^{3+}$[a]

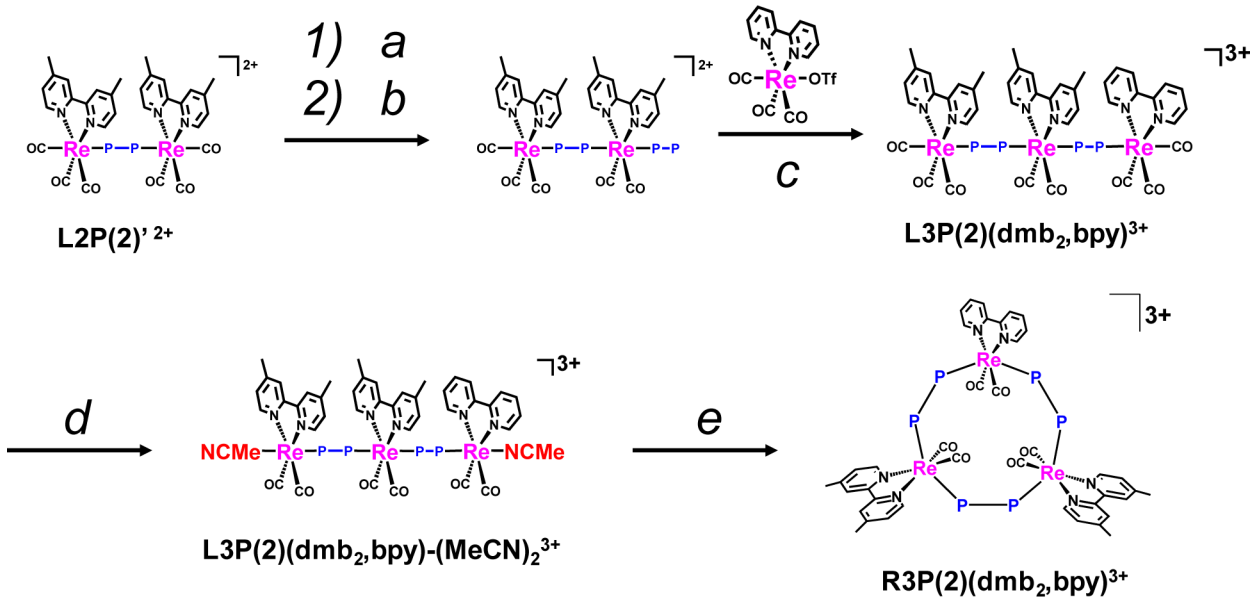

[a](a) *hv* (> 330 nm) in CH_2Cl_2 for 25 min; (b) **P(2)** (3 equiv), reflux in CH_2Cl_2 for 2 d; (c) Re(bpy)$(CO)_3(CF_3SO_3)$ (1.2 equiv), reflux in THF for 1 d; (d) *hv* (> 330 nm) in acetone−water (10:1 v/v) for 6 h, then addition of MeCN; and (e) **P(2)** (1.1 equiv), reflux in acetone for 15.5 h, and then addition of MeOH containing NH_4PF_6.

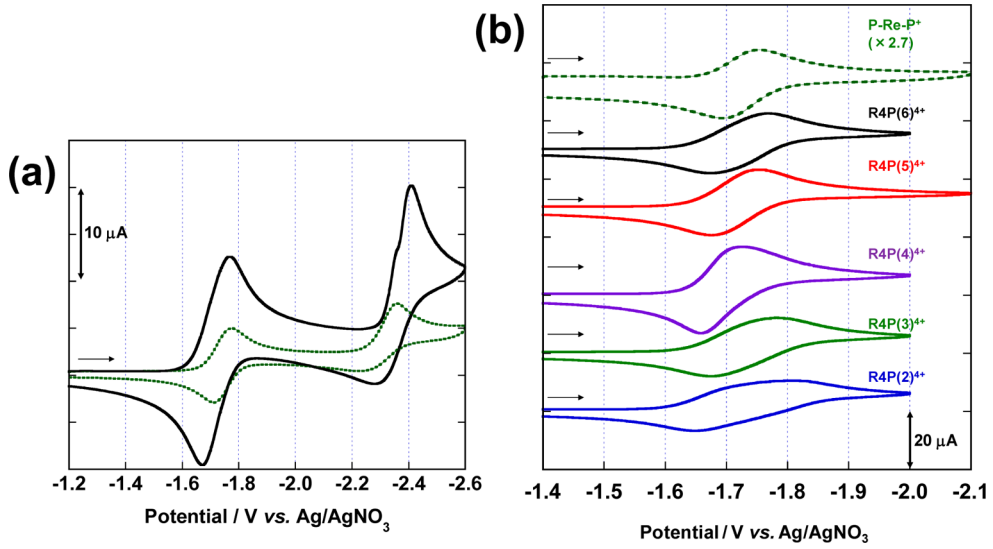

Figure 2. Voltammograms of **P−Re−P**$^+$ and ring-shaped multinuclear complexes measured in DMF containing 0.1 M Et_4NBF_4 at room temperature. (a) **P−Re−P**$^+$ (green dotted line) and **R4P(6)**$^{4+}$ (black line); (b) **P−Re−P**$^+$ (green dotted line), **R4P(2)**$^{4+}$ (blue line), **R4P(3)**$^{4+}$ (green line), **R4P(4)**$^{4+}$ (purple line), **R4P(5)**$^{4+}$ (red line), and **R4P(6)**$^{4+}$ (black line).

shaped multinuclear complexes with different Re units that are difficult to synthesize by the previously reported method. Scheme 2 illustrates the synthetic procedures of a ring-shaped trinuclear complex composed of two Re units with a 4,4′-dimethyl-2,2′-bipyridine (dmb) ligand and one with a bpy ligand (**R3P(2)(dmb$_2$,bpy)**$^{3+}$).

The corresponding linear-shaped trinuclear complex **L3P-(2)(dmb$_2$,bpy)**$^{3+}$, which was used as a starting complex, was synthesized by the previously reported method using **L2P(2)**$'^{2+}$ with dmb ligands and Re(bpy)$(CO)_3(CF_3SO_3)$.[10,12] An acetone−water mixture containing **L3P(2)(dmb$_2$,bpy)**$^{3+}$ was irradiated, yielding the photochemical-ligand-substitution product **L3P(2)(dmb$_2$,bpy)-(Sol)$_2$**$^{3+}$ (Supporting Information, Figure S3). Thermal reaction of **L3P(2)(dmb$_2$,bpy)-(MeCN)$_2$**$^{3+}$(which was obtained by the ligand substitution with MeCN) with **P(2)** afforded **R3P(2)(dmb$_2$,bpy)**$^{3+}$ in a 17% isolated yield based on the **L2P(2)**$'^{2+}$ used in the procedure.

Electrochemical Properties. Figure 2a shows the cyclic voltammogram (CV) of **R4P(6)**$^{4+}$ measured in dimethylformamide (DMF). One reversible wave and another irreversible wave were observed at $E_{1/2}$ = −1.72 V and E_p = −2.34 V versus $Ag/AgNO_3$, respectively, which are attributed to reduction of the ligand (bpy/bpy$^-$·) and rhenium (Re^I/Re^0), respectively.[8] Although these potentials were similar to those of the model mononuclear complex $[Re(bpy)(CO)_2(PPh_2Pr)_2]^+$ (**P−Re−P**$^+$ in Chart 1; $E_{1/2}$ = −1.73 V and E_p = −2.36 V), the observed current with **R4P(6)**$^{4+}$ was 2.7-fold higher than that of **P−Re−**

dx.doi.org/10.1021/ic501196q | Inorg. Chem. 2014, 53, 7170−7180

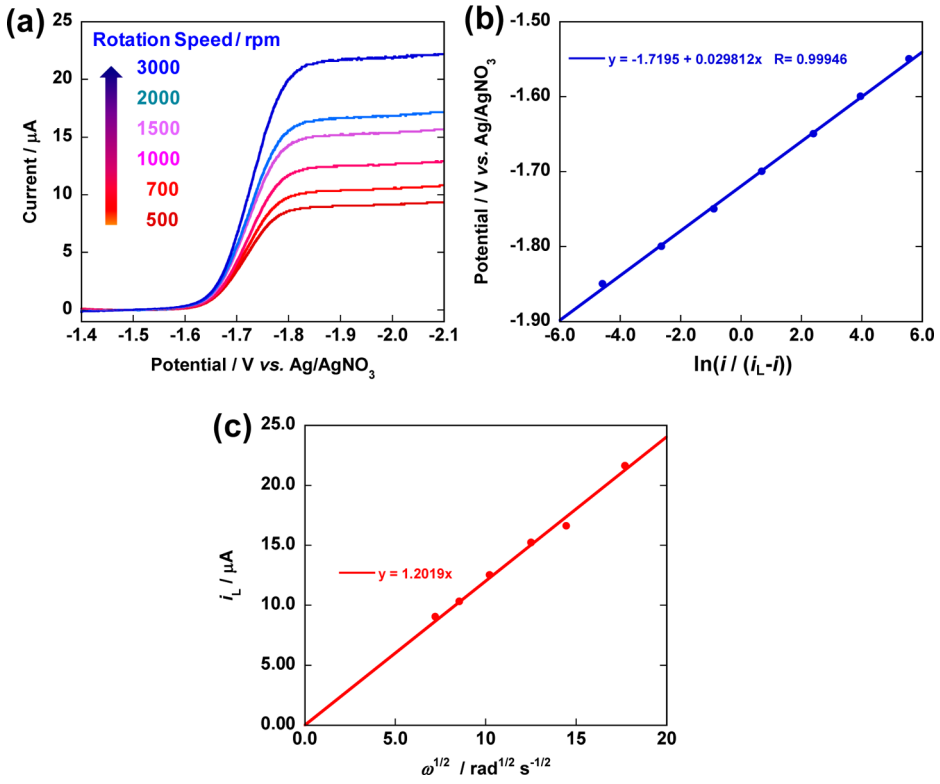

Figure 3. (a) Hydrodynamic voltammograms of **R4P(6)**$^{4+}$ (0.125 mM) measured using a rotating disk electrode in DMF containing Et_4NBF_4 (0.1 M) as a supporting electrolyte with a $Ag/AgNO_3$ reference electrode under an Ar atmosphere at different rotation speeds (500, 700, 1000, 1500, 2000, and 3000 rpm). (b) Logarithmic plots of the current vs potentials at 2000 rpm. (c) Levich plot.

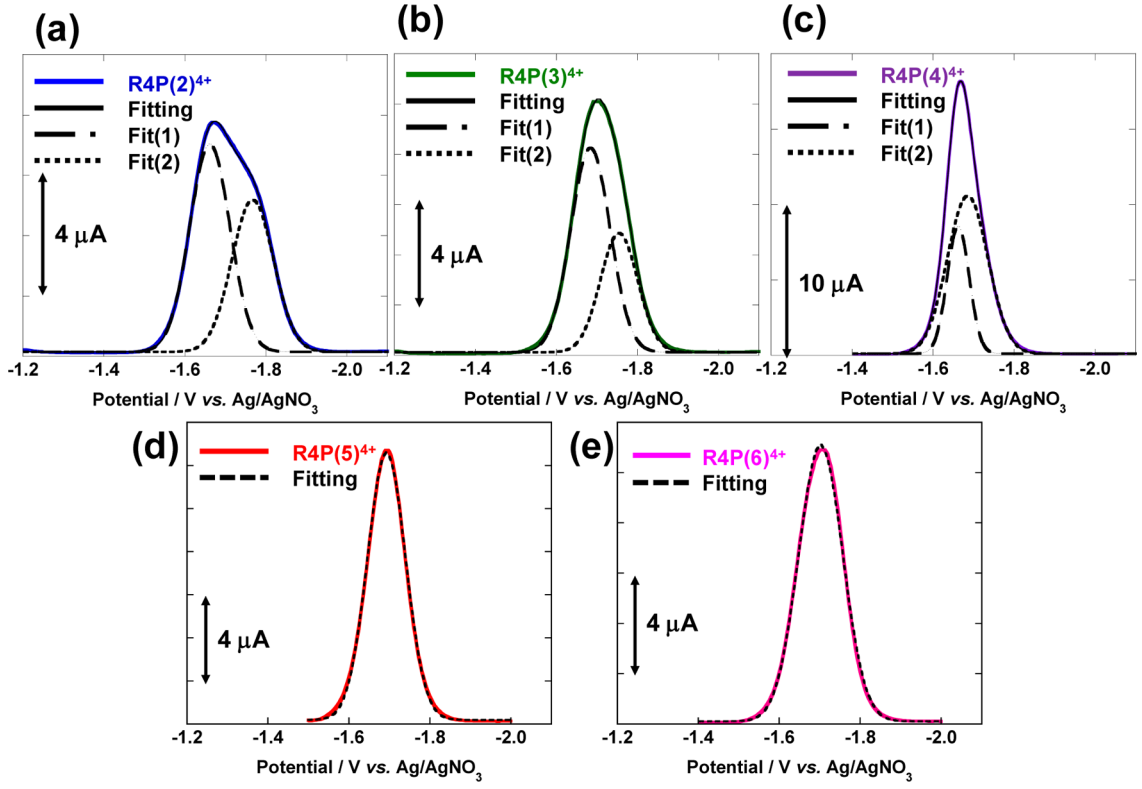

Figure 4. Differential pulse voltammograms of (a) **R4P(2)**$^{4+}$(blue), (b) **R4P(3)**$^{4+}$(green), (c) **R4P(4)**$^{4+}$(purple), (d) **R4P(5)**$^{4+}$(red), and (e) **R4P(6)**$^{4+}$(pink) recorded in DMF solutions containing Et_4NBF_4 (0.1 M) as the supporting electrolyte. Fitting results using one or two Gaussian function(s) are represented by black lines.

dx.doi.org/10.1021/ic501196q | Inorg. Chem. 2014, 53, 7170−7180

$\mathbf{P}^+$ at a scan rate of 100 mV s^{-1}. Using eq 9, which is applicable to molecules containing multiple noninteracting redox centers,[13] the number of electrons accepted by one molecule of $\mathbf{R4P(6)}^{4+}$ (n_p) was obtained to be ca. four.

$$n_p = \frac{(i_p/C_p)}{(i_m/C_m)}(M_p/M_m)^{0.275} \quad (9)$$

where M, C, and i are molecular weights, concentration, and current, respectively (subscript "m" represents $\mathbf{P-Re-P}^+$, while "p" represents $\mathbf{R4P(6)}^{4+}$).[13] This result was also consistent with the results from the bulk electrolysis experiment performed using the flow electrolysis technique (Supporting Information, Figure S4), that is, analysis of the data indicated that ca. four electrons were accepted by one molecule of $\mathbf{R4P(6)}^{4+}$ at potentials more negative than −2 V.

Figure 3a illustrates the hydrodynamic voltammograms of $\mathbf{R4P(6)}^{4+}$ (0.125 mM) measured using a rotating disk electrode. Application of eq 10 to the results illustrated in Figure 3b also indicated that all four Re units in $\mathbf{R4P(6)}^{4+}$ could independently accept one electron at the same potential, that is, $\mathbf{R4P(6)}^{4+}$ is constructed with noninteracting redox centers, because n was 1,[13] and the linearity of the Levich plots (Figure 3c) indicates that the reduced species was stable on the time scale of the measurement.

$$E = E_{1/2} + (RT/nF)\ln[(i)/(i_L - i)] \quad (10)$$

where i_L and i are limiting and background current, respectively, and n is the number of electrons accepted by each Re unit of $\mathbf{R4P(6)}^{4+}$.

Another interesting difference between the CVs of $\mathbf{R4P(6)}^{4+}$ and $\mathbf{P-Re-P}^+$ was the exclusive presence of a shoulder in the second reduction wave of $\mathbf{R4P(6)}^{4+}$ (Figure 2a). This shoulder became more evident at a slower scan rate (Supporting Information, Figure S5), and this phenomenon was observed only in the case of $\mathbf{R4P(6)}^{4+}$; however, we could not rationalize it.

Figure 2b shows the first redox waves of all synthesized ring-shaped tetranuclear complexes for comparison. The voltammogram of $\mathbf{R4P(5)}^{4+}$ was similar to that of $\mathbf{R4P(6)}^{4+}$; in contrast, the reduction wave in the voltammogram of $\mathbf{R4P(4)}^{4+}$ was broader than that of $\mathbf{R4P(6)}^{4+}$. The shorter alkyl chains ($x \leq 4$) in the bidentate phosphorus ligands caused the broader reduction wave of $\mathbf{R4P(x)}^{4+}$. In particular, two distinct reduction peaks were observed in the case of $\mathbf{R4P(2)}^{4+}$ (−1.66 V, −1.76 V). Figure 4 illustrates differential pulse voltammograms (DPVs) of the ring-shaped tetranuclear complexes in the region of the first reduction wave(s). Although the DPVs of $\mathbf{R4P(5)}^{4+}$and $\mathbf{R4P(6)}^{4+}$ could be fitted using a single Gaussian function (Figure 4d,e), a linear combination of two Gaussian functions was required in the cases of the ring-shaped multinuclear complexes with shorter alkyl chains, namely, $\mathbf{R4P(2)}^{4+}$, $\mathbf{R4P(3)}^{4+}$, and $\mathbf{R4P(4)}^{4+}$ (Figure 4a,b,c). These results indicated the onset of weak electronic interaction between the Re units in the ring-shaped tetranuclear complexes with relatively short bridging ligands. This could likely be attributed to the initial reduction of two Re units, positioned at opposing sites, at a more positive potential, followed by the reduction of the other two units at more negative potentials owing to the interaction with the adjacent reduced units. The influence of such intramolecular interactions in the tetranuclear complexes should be more evident when the Re(I) units are linked with shorter alkyl chains. On the other hand, the shape and potential of the first reduction wave of the hexanuclear complex $\mathbf{R6P(4)}^{6+}$ (Supporting Information, Figure S6a) was similar to that of $\mathbf{R4P(5)}^{4+}$ or $\mathbf{R4P(6)}^{4+}$, and its DPV could be fitted with a single Gaussian function (Supporting Information, Figure S6b). Therefore, higher number of Re units within a ring-shaped structure resulted in weakening of the electronic interaction between the Re units, which could likely be attributed to loss in rigidity of the structure. Table 2 summarizes the electrochemical data of the ring-shaped multinuclear complexes and the model mononuclear complex.

Table 2. Electrochemical Data of the Ring-Shaped Re(I) Multinuclear Complexes and $\mathbf{P-Re-P}^+$

	E (V) vs $Ag/AgNO_3$ (ΔE_p (mV))[a]	
complex	$E_{1/2}$ (bpy/bpy$^{\bullet-}$)	E_p (Re^I/Re^0)
$\mathbf{R4P(2)}^{4+}$	−1.66, −1.76[b]	−2.29[c]
$\mathbf{R4P(3)}^{4+}$	−1.68, −1.75[b]	−2.33
$\mathbf{R4P(4)}^{4+}$	−1.66, −1.69[b]	−2.34
$\mathbf{R4P(5)}^{4+}$	−1.69 (77)	−2.37
$\mathbf{R4P(6)}^{4+}$	−1.72 (90)	−2.34
$\mathbf{R6P(4)}^{6+}$	−1.68 (90)	−2.32
$\mathbf{P-Re-P}^+$	−1.73 (60)	−2.36

[a]Measured in DMF containing 0.1 M Et_4NBF_4 at room temperature using a glassy carbon disc working electrode and a Pt-wire counter electrode. [b]See Figure 4 for details. [c]The reduced complex was adsorbed on the working electrode.

Photochemical Multielectron Accumulation. Since the ring-shaped tetranuclear complexes were photochemically stable and their lowest triplet of metal-to-ligand charge-transfer (^{3}MLCT) excited states had lifetimes of several hundred nanoseconds, we investigated the photochemical behaviors of $\mathbf{RnP(x)}^{n+}$ in the presence of a sacrificial electron donor, namely, TEOA. As a typical example, Figure 5a shows the UV−vis absorption spectra of a DMF−TEOA (5:1 v/v) mixed solution containing $\mathbf{R4P(4)}^{4+}$ (0.05 mM) during irradiation at λ = 436 nm (2.1×10^{-7} einstein s^{-1}) at various irradiation times for a maximum of 20 min. The differential absorption spectra derived from the spectrum before irradiation and the spectra after irradiation (Figure 5b) exhibit new absorption bands at λ_{max} = 361, 484, and 518 nm, which are very similar to the differential absorption spectrum of the OERS of $\mathbf{P-Re-P}^+$ derived from the absorption spectra obtained before and after flow electrolysis (Figure 5c and Supporting Information, Figure S7b).

This result indicates that the OERS of the Re unit(s) in $\mathbf{R4P(4)}^{4+}$ were accumulated in the reaction solution during irradiation. Similar results were obtained in the cases of the other ring-shaped tetranuclear complexes (Supporting Information, Figure S8).[14] Using the molar extinction coefficient of the OERS of the corresponding mononuclear complex $\mathbf{P-Re-P}^+$ (ε_{550} = 1760 M^{-1} cm^{-1}, Supporting Information, Figure S7), the number of average electrons accumulated in one molecule of $\mathbf{RnP(x)}^{n+}$ (N) was estimated by means of eqs 11 and 12 as follows:

$$N = \frac{C_{red}}{C_{ring}} \quad (11)$$

dx.doi.org/10.1021/ic501196q | Inorg. Chem. 2014, 53, 7170−7180

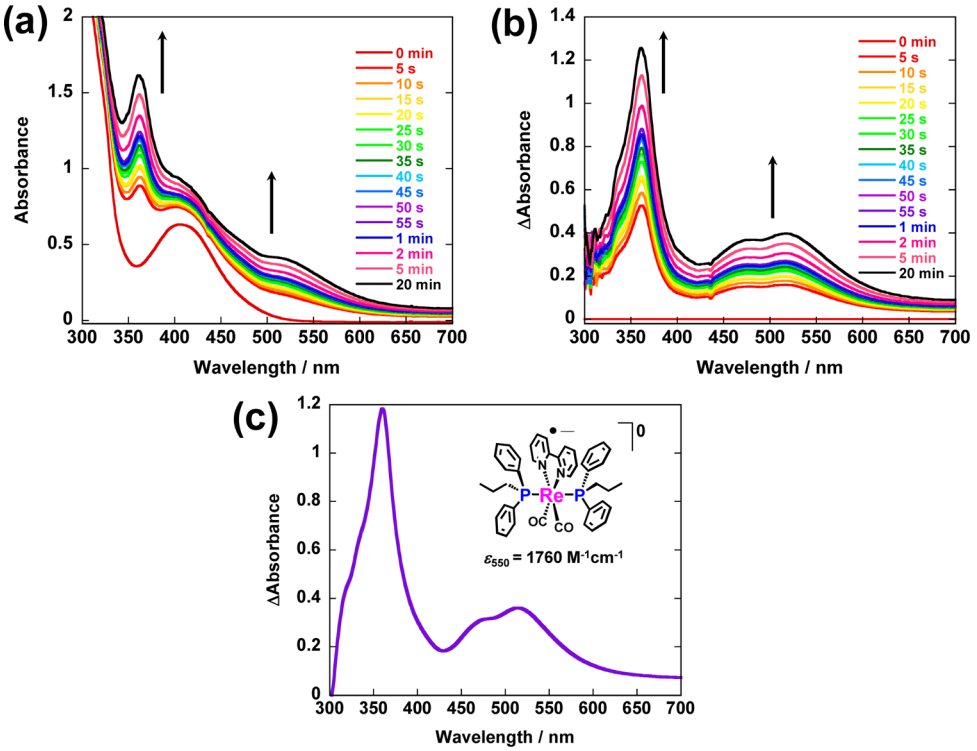

Figure 5. (a) UV−vis absorption spectra of a DMF−TEOA (5:1 v/v) solution containing **R4P(4)**$^{4+}$ (0.05 mM) for irradiation at λ = 436 nm (2.1×10^{-7} einstein s^{-1}) at various irradiation times for a maximum of 20 min. (b) Differential absorption spectra derived from the spectrum before irradiation and the spectra after irradiation. (c) The differential absorption spectrum of the OERS of **P−Re−P**$^{+}$ derived from the absorption spectra obtained before and after flow electrolysis (Supporting Information, Figure S7).

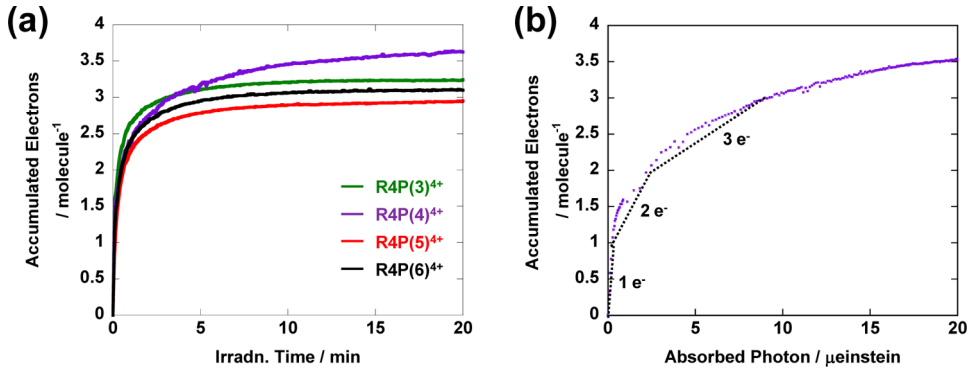

Figure 6. (a) Time courses of accumulated electrons in each **R4P(*x*)**$^{4+}$ molecule, given as **R4P(3)**$^{4+}$ (green), **R4P(4)**$^{4+}$ (purple), **R4P(5)**$^{4+}$ (red), and **R4P(6)**$^{4+}$ (black) during 436 nm irradiation (2.1×10^{-7} einstein s^{-1}) in DMF−TEOA (5:1 v/v). (b) Time course of accumulated electrons in **R4P(4)**$^{4+}$ compensated for the inner filter effect (see Supporting Information). The average quantum yields of the first, second, and third electron accumulations were obtained using the dotted lines.

$$C_{red} = \frac{A_{550}}{\varepsilon_{550} \cdot d} \tag{12}$$

where C_{red}, C_{ring}, A_{550}, and d are concentration of the reduced Re units, concentration of the added **RnP(*x*)**$^{n+}$, change in absorbance at 550 nm, and pass length (1 cm), respectively. Figure 6a shows the dependence of N on the irradiation time. Notably, one molecule of **R4P(*x*)**$^{4+}$ could accumulate 2.9−3.6 electrons after 20 min of irradiation (Table 3). The absorption spectrum of the irradiated solution after it was exposed to the air was very similar to that before irradiation (Supporting Information, Figure S9). This information clearly shows that all or most Re(I) units in **R4P(*x*)**$^{4+}$ can be photochemically reduced in the presence of TEOA, and these multielectron reduced species are stable in the solution for at least several tens of minutes. We applied photochemical multielectron reduction to the hexanuclear complex **R6P(4)**$^{6+}$. The spectral changes were very similar to those observed for **R4P(4)**$^{4+}$, and the number of accumulated electrons in one molecule increased to 4.4 electrons for 25 min of irradiation, and the reduced **R6P(4)**$^{6+}$ was also stable (Supporting Information, Figures S10 and S11).

For determining the average formation quantum yields of the OERS of the Re units in the ring-shaped multinuclear complex after one or more of the Re unit(s) have already accepted an electron, the inner filter effect of the reduced units should be eliminated because the reduced unit exhibits strong absorption over a wide range of the visible region, and the excited state of

dx.doi.org/10.1021/ic501196q | Inorg. Chem. 2014, 53, 7170−7180

Table 3. Number of Accumulated Electrons in One Complex, Average Quantum Yields of Each Electron Accumulation Process, Lifetimes, and Stern–Volmer Constants

	accumulated electrons	Φ_{OERS} (%)				K_{sv}[b]
complex	molecule^{-1}	1st	second	third	τ (ns)[a] (A_i (%))	M^{-1}
R4P(3)$^{4+}$	3.2	123	40	4.7	227, 491 (56.3), (43.7)	0.34
R4P(4)$^{4+}$	3.6	77	10	2.9	177, 644 (73.4), (26.6)	0.15
R4P(5)$^{4+}$	2.9	66	7	0.8	185, 854 (82.5), (17.5)	0.77
R4P(6)$^{4+}$	3.1	90	9	1.5	248, 527 (22.9), (77.1)	1.26
R6P(4)$^{6+c}$	4.4	32	15	5	166, 661 (76.6), (23.4)	1.21

[a]Measured in MeCN from ref 7b. The emission decay curves were fitted by a double exponential function ($I = A_1 \exp(t/t_1) + A_2 \exp(t/t_2)$), and percentages of pre-exponential factors a_i was defined as $100A_i/(A_1 + A_2)$ (i = 1, 2). [b]Stern–Volmer constants obtained from quenching experiments of emission by TEOA (Supporting Information, Figure S13). K_{sv} of **R4P(2)**$^{4+}$ was 1.83 M^{-1}. [c]The average quantum yield of accumulation of the fourth electron was 0.6%.

the reduced unit should quickly decay (see Supporting Information). As a typical example, Figure 6b shows the dependence of N for **R4P(4)**$^{4+}$ on the number of absorbed photons by nonreduced Re units, which has been already compensated for the inner filter effect. Using this result, the average quantum yields of the first, second, and third processes of electron-accumulation into **R4P(4)**$^{4+}$ (Φ_{OERS}) were estimated as 77%, 10%, and 2.9%, respectively. The first electron-accumulation process was very efficient, while the second and third processes were gradually less efficient. This was not completely unexpected, as the OER unit in the reduced ring-shaped multinuclear complex could be an efficient electron donor to another excited Re unit in the same ring-shaped multinuclear complex. In other words, intramolecular electron transfer from the OER unit to the excited Re unit was the most likely deactivation pathway for the excited state of the Re unit in the reduced ring-shaped multinuclear complexes with 1–3 extra electron(s). However, multiple electrons could still be accumulated in all ring-shaped multinuclear complexes owing to potentially weak electronic interaction among Re units in the ring-shaped multinuclear complexes.

Similar results were obtained in the cases of the other **R4P(x)**$^{4+}$ and **R6P(4)**$^{6+}$ (Table 3, Figure 6a and Supporting Information, Figure S12). It is worth noting that TEOA can photochemically donate two electrons because the α-amino radical, TEOA$^{+\bullet}$, which was produced by photochemical oxidation by the excited ring-shaped multinuclear complex, can serve as a one-electron donor.[2d] Thus, a value for Φ_{OERS} that was greater than 100% for **R4P(3)**$^{4+}$ is not surprising. The Φ_{OERS} values of the first reduction process were different for different ring-shaped multinuclear complexes, whereas the number of accumulated electrons in each molecule was similar (Table 3). Quenching of the excited ring-shaped multinuclear complex by TEOA, that is, the initial step of the photochemical redox reaction, should affect Φ_{OER}. It has been reported that there are at least two conformers of the excited ring-shaped multinuclear complexes that present distinct π–π interactions and possess different lifetimes in solution. As the distribution of the conformers strongly depended on solvent polarity, and both the oxidation power and the emission quantum yield of the excited ring-shaped multinuclear complexes were also affected by the π–π interaction,[7b] the kinetics of the quenching process could not be analyzed directly. However, the Stern–Volmer treatment (Supporting Information, Figure S13) offered relative rates of quenching of the excited ring-shaped multinuclear complexes by TEOA. The Stern–Volmer constants (K_{SV}) are summarized in Table 3. Surprisingly, a distinct relationship between the Stern–Volmer constant and Φ_{OERS} could not be established. Therefore, other factors, such as an escape yield from a solvent cage and rate of back electron transfer from the reduced ring-shaped multinuclear complex to TEOA$^{+\bullet}$ before and/or after the escaping could account for the ring-shaped multinuclear complex-dependent differences in the electron accumulation rates.

EXPERIMENTAL SECTION

General Procedures. IR spectra were recorded on a JASCO Fourier transform infrared (FT-IR) spectrometer at 1 cm^{-1} resolution. UV–vis absorption spectra were recorded on a JASCO V-565 spectrophotometer or a Photal MCPD-2000 photodiode array spectrometer. ^1H NMR spectra were recorded on a JEOL AL300 (300 MHz) or AL400 (400 MHz) spectrometer. The residual protons of acetone-d_6 or CD_3CN were used as an internal standard for the measurements. ESI-MS was performed with a Shimadzu LCMS-2010A system with MeCN or MeOH as the mobile phase. Electrospray ionization time-of-flight mass spectroscopy (ESI-TOFMS) was undertaken with a Waters LCT Premier, with acetonitrile as a mobile phase. Emission spectra were measured at (25 ± 0.1) °C with a JASCO FP-6500 spectrofluorometer. Emission lifetimes were measured with a Horiba NAES-1100 time-correlated single-photon-counting system (the excitation source was a nanosecond H_2 lamp, NFL-111, and the instrument response time was <1 ns) or a Horiba FluoroCube time-correlated single-photon counting system (the excitation source was an LED pulse lamp (λ = 401 nm), and the instrumental response time was <200 ps). The samples were degassed by the freeze–pump–thaw method before the emission measurements. The redox potentials of the complexes were measured in a DMF solution containing Et_4NBF_4 (0.1 M) as a supporting electrolyte using an ALS/CHI CHI-620 electrochemical analyzer with a glassy carbon disc working electrode (3 mm diameter), a $Ag/AgNO_3$ (0.01 M) reference electrode, and a Pt counter electrode. The supporting electrolyte was dried in vacuo at 100 °C for 1 d prior to use. The scan rate was 100 mV s^{-1}. The hydrodynamic voltammograms of the complexes (**P–Re–P**$^+$(PF_6^-): 0.5 mM; **R4P(6)**$^{4+}$(PF_6^-)$_4$: 0.125 mM) were measured in a DMF solution containing Et_4NBF_4 (0.1M) as a supporting electrolyte by hydrodynamic voltammetric techniques, using a RRDE-3A rotating ring disc electrode rotator (BAS Co., Ltd.), an ALS/CHI CHI-720Dx electrochemical analyzer with a glassy-carbon rotating ring disc electrode (4 mm diameter) as a working

dx.doi.org/10.1021/ic501196q | Inorg. Chem. 2014, 53, 7170–7180

electrode, a $Ag/AgNO_3$ (0.01M) reference electrode, and a Pt counter electrode. The supporting electrolyte was dried in vacuum at 100 °C for 1 d prior to use. The scan rate was 20 mV s^{-1}. The method of flow electrolysis has been described in detail elsewhere.[2b] Separation of the Re(I) multinuclear complexes was achieved by size-exclusion chromatography (SEC)[10,15] using a JAI LC-9201 preparative recycle HPLC apparatus with two sequentially connected Shodex PROTEIN KW-2002.5 columns (300 mm × 20.0 mm i.d.), a KW-LG guard column (50 mm × 8.0 mm i.d.), and a JASCO 870-UV detector. The eluent was a 1:1 (v/v) mixture of MeOH and MeCN containing 0.15 M $CH_3CO_2NH_4$. For analysis by SEC, we used two sequentially connected Shodex KW-402.5−4F (300 mm × 4.6 mm i.d.) with a KW400G-4A guard-column (10 mm × 4.6 mm i.d.), a JASCO 880−51 degasser, a 880-PU pump, a MD-2010 Plus UV−vis photodiode-array detector, and a Rheodyne 7125 injector. The detection wavelength was chosen as 360 nm because all of the complexes analyzed have strong MLCT and/or $\pi-\pi^*$ absorption bands around 350−500 nm. The column temperature was maintained at (40 ± 1) °C using a JASCO 860-CO column-oven. The eluent was a 1:1 (v/v) mixture of MeOH and MeCN containing 0.5 M $CH_3CO_2NH_4$, and the flow rate was 0.2 mL min^{-1}.

Materials. MeCN was distilled three times over P_2O_5 and then distilled over CaH_2 immediately before use. THF was distilled from benzophenone ketyl under nitrogen before use. CH_2Cl_2 was distilled over calcium hydride after drying on calcium chloride. DMF was dried over molecular sieves (4Å) and distilled under reduced pressure before use. All other reagents were reagent-grade quality and were used without further purification.

For the photochemical ligand substitution reactions, the solution was irradiated with an Eikosha EHBWI-500 high-pressure mercury lamp (500 W) with a uranium glass filter (>330 nm) in a Pyrex donut-form vessel. During irradiation, the solution was bubbled with a N_2 or Ar gas, and the vessel was cooled with tap water.

The ring-shaped trinuclear, tetranuclear, and hexanuclear Re(I) complexes (Chart 1) were also synthesized as PF_6^- salts by the following procedures.

***R3P(2)*$^{3+}$*$(PF_6^-)_3$.** An acetone−H_2O (7:1 v/v) mixed solution (160 mL) containing **L3P(2)**$^{3+}(PF_6^-)_3$ (51.65 mg, 0.020 mmol) was irradiated for 6 h under a N_2 atmosphere. After the solvent was evaporated, MeCN (100 mL) was added, and then the solution was evaporated again. This process was repeated several times until the red precipitate was obtained. An acetone solution (60 mL) containing the crude product and **P(2)** (9.10 mg, 0.023 mmol) was refluxed for 15 h under a N_2 atmosphere in dim light. After the solution was evaporated, the residue was separated using SEC. The eluted solutions containing the product were evaporated, and the residue was extracted using CH_2Cl_2 and water containing NH_4PF_6. After the organic phase was evaporated, the residue was dissolved into a small amount of MeOH. NH_4PF_6-saturated MeOH and a small amount of H_2O were added into the solution. Slow evaporation of the solution precipitated the target complex with a yield of 34% (19.8 mg) based on **L3P-(2)**$^{3+}(PF_6^-)_3$ used.

***R4P(2)*$^{4+}$*$(PF_6^-)_4$.** An acetone−H_2O (v/v = 7:1) mixture (120 mL) containing **L4P(2)**$^{4+}(PF_6^-)_4$ (53.8 mg, 0.015 mmol) was irradiated for 3.5 h under a N_2 atmosphere. After the solvent was evaporated, MeCN (100 mL) was added, and then evaporated again. This process was repeated several times until the red precipitate was obtained. An acetone solution (60 mL) of the crude product and **P(2)** (6.3 mg, 0.016 mmol) was refluxed for 18 h under a N_2 atmosphere in dim light. After the solvent was evaporated, the residue was washed with acetone containing $CH_3CO_2NH_4$ (0.15 M). The yellow precipitate was dissolved into a small amount of MeOH. An NH_4PF_6 saturated MeOH and a small amount of H_2O was added to the solution. The precipitated yellow powder was washed with H_2O and diethyl ether with a yield of 51% (30.0 mg) based on **L4P(2)**$^{4+}(PF_6^-)_4$ used.

A similar synthetic procedure was applied to the other tetranuclear complexes except for the isolation method, as described below. The yields were based on the corresponding linear-shaped Re multinuclear complex.

***R4P(3)*$^{4+}$*$(PF_6^-)_4$.** Yield 39%. After the reaction mixture was evaporated, acetone was added to the residue. The yellow precipitate was washed with diethyl ether.

***R4P(4)*$^{4+}$*$(PF_6^-)_4$.** Yield 58%. After the reaction mixture was evaporated, the residue was recrystallized with THF. The orange precipitate was washed with diethyl ether.

***R4P(5)*$^{4+}$*$(PF_6^-)_4$.** Yield 64%. After the reaction mixture was evaporated, the residue was separated using SEC. The eluted solutions containing the product were evaporated. The residue was extracted using CH_2Cl_2 and water containing NH_4PF_6. After the organic phase was evaporated, the residue was dissolved into a small amount of MeOH. NH_4PF_6 saturated MeOH and a small amount of H_2O were added into the solution. Slow evaporation of the solution precipitated the target complex.

***R4P(6)*$^{4+}$*$(PF_6^-)_4$.** Yield 109.5 mg (70%). After the reaction mixture was evaporated, acetone was added to the residue. The orange precipitate was washed with diethyl ether.

***R6P(4)*$^{6+}$*$(PF_6^-)_6$.** An acetone−H_2O (7:1 v/v) mixture (400 mL) containing **L6P(4)**$^{6+}(PF_6^-)_6$ (186.95 mg, 34.7 μmol) was irradiated for 2 h under a N_2 atmosphere. After the solvent was evaporated, MeCN (100 mL) was added into the residue, and then the solution was evaporated again. This process was repeated several times until the red precipitate was obtained. The red precipitate was dissolved into 60 mL of acetone, and 8.00 mg of **P(4)** was added to the solution. After the solution was heated at 50 °C for 1 d, 8.85 mg of **P(4)** was added. The same cycle was repeated again with 8.90 mg of **P(4)**; therefore, 60.3 μmol of **P(4)** was added into the reaction solution in total, and the reaction solution was heated for 3 d in total. After the solution was evaporated, the residue was separated using SEC. The eluted solutions containing the product were evaporated, and the residue was extracted using CH_2Cl_2 and water containing NH_4PF_6. After the organic phase was evaporated, the residue was dissolved into a small amount of CH_3OH. NH_4PF_6-saturated CH_3OH and a small amount of H_2O were added into the solution. Slow evaporation of the solution precipitated the target complex with a yield of 34% (67.8 mg) based on **L6P(4)**$^{6+}(PF_6^-)_6$ used.

***L3P(2)(dmb$_2$,bpy)*$^{3+}$*$(PF_6^-)_3$.** A CH_2Cl_2 solution (200 mL) containing **L2P(2)**$'^{2+}(CF_3SO_3^-)_2$ (199.6 mg, 0.124 mmol) was irradiated for 25 min under a N_2 atmosphere. **P(2)** (148.7 mg, 0.373 mmol) was added to the reaction solution, and it was refluxed for 2 d under a N_2 atmosphere in dim light. After the solvent was evaporated, the residue was recrystallized with CH_2Cl_2−diethyl ether−*n*-hexane for removal of the remaining **P(2)**. The yellow powder was washed with diethyl ether and dried in vacuo, yielding roughly purified $[Re(dmb)(CO)_3\text{-}(\mu_2\text{-}\mathbf{P(2)})\text{-}Re(dmb)(CO)_2(\eta^1\text{-}\mathbf{P(2)})](CF_3SO_3^-)_2$ (246.2 mg). ESI-MS (in MeCN) *m*/*z*: 839 $[M - 2CF_3SO_3]^{2+}$. The complex (246.2 mg) was dissolved in THF (20 mL) containing *fac*-$Re(bpy)(CO)_3(CF_3SO_3)$ (109.1 mg, 0.190 mmol), and the solution was refluxed under a N_2 atmosphere for 1 d in dim light. After the solvent was evaporated, the residue was separated using SEC. The eluted solutions containing the product were evaporated, and the residue was extracted using CH_2Cl_2 and water containing NH_4PF_6. After the organic phase was evaporated, the residue was dissolved into a small amount of MeOH. NH_4PF_6-saturated MeOH and a small amount of H_2O were added into the solution. Slow evaporation of the solution precipitated the target complex with a yield of 59% (184.6 mg) based on the **L2P(2)**$'^{2+}(CF_3SO_3^-)_2$ used. ^1H NMR (300 MHz, acetone-d_6): 8.85 (d, 2H, *J* = 5.3 Hz, bpy-6,6′), 8.64 (d, 2H, *J* = 5.7 Hz, edge-dmb-6,6′), 8.29 (d, 2H, *J* = 7.8 Hz, bpy-3,3′), 8.20 (t, 2H, *J* = 7.8 Hz, bpy-4,4′), 8.14 (s, 2H, edge-dmb-3,3′), 8.04 (d, 2H, *J* = 5.7 Hz, interior-dmb-6,6′), 7.74 (s, 2H, interior-dmb-3,3′), 7.64 (dd, 2H, *J* = 5.3, 7.8 Hz, bpy-5,5′), 7.55−7.42 (m, 10H, edge-dmb-5,5′, Ph-*p*), 7.35−7.28 (m, 16H, Ph-*m*), 6.97 (d, 2H, *J* = 5.7, interior-dmb-5,5′), 6.89−6.80 (m, 16H, Ph-*o*), 2.55 (s, 6H, edge-C$\underline{H}_3$), 2.39 (s, 6H, interior-C$\underline{H}_3$), 1.86−1.76 (m, 8H, $PPh_2\text{-}(C\underline{H}_2)_2\text{-}Ph_2P$). FT-IR (in CH_2Cl_2) ν_{CO}/cm^{-1}: 2040, 1955, 1935, 1921, 1862 cm^{-1}. ESI-MS (in MeCN) *m*/*z*: 701 $[M - 3PF_6]^{3+}$.

***R3P(2)(dmb$_2$,bpy)*$^{3+}$*$(PF_6^-)_3$.** An acetone−water mixture (10:1 v/v, 330 mL) containing **L3P(2)(dmb$_2$,bpy)**$^{3+}(PF_6^-)_3$ (104.9 mg, 0.0413 mmol) was irradiated for 6 h under a N_2 atmosphere. After the solvent

dx.doi.org/10.1021/ic501196q | Inorg. Chem. 2014, 53, 7170−7180

was evaporated, MeCN (100 mL) was added into the residue, and then the solution was evaporated again. These processes were repeated several times until the red precipitate was obtained. The residue was recrystallized with CH_2Cl_2−*n*-hexane, primarily yielding **L3P(2)-(dmb$_2$,bpy)-(MeCN)$_2$**$^{3+}$ (102.5 mg), which was used in the following process without further purification. ESI-MS (in CH_2Cl_2) *m*/*z*: 710 [**L3P(2)(dmb$_2$,bpy) -(MeCN)$_2$**]$^{3+}$; 706 [**L3P(2)(dmb$_2$,bpy)-(MeCN)**]$^{3+}$. FT-IR (in CH_2Cl_2) ν_{CO}/cm^{-1}: 1939, 1866 (sh), 1858. An acetone solution (40 mL) containing the crude **L3P(2)-(dmb$_2$,bpy)-(MeCN)$_2$**$^{3+}$ and **P(2)** (16.4 mg, 0.041 mmol) was refluxed for 15.5 h under a N_2 atmosphere in dim light. After the solvent was evaporated, the residue was separated using SEC. The eluted solutions containing the product were evaporated. The residue was extracted using CH_2Cl_2 and water containing NH_4PF_6. After the organic phase was evaporated, the residue was dissolved with a small amount of MeOH. NH_4PF_6-saturated MeOH and a small amount of H_2O were added into the solution. Slow evaporation of the solution precipitated the target complex (29%, 33.9 mg). The yield was based on the **L3P(2)(dmb$_2$,bpy)**$^{3+}$(PF_6^-)$_3$ used. ^{1}H NMR (300 MHz, CD_3CN): δ (ppm) = 8.55 (d, 2H, *J* = 5.6 Hz, bpy-6,6′), 8.40 (d, 4H, *J* = 5.6 Hz, dmb-6,6′), 7.70−7.59 (m, 4H, bpy-4,4′, bpy-3,3′), 7.40 (s, 4H, dmb-3,3′), 7.29−7.24 (m, 12H, Ph-*p*), 7.12−7.06 (m, 26H, bpy-5,5′, Ph-*m*), 6.95 (d, 4H, *J* = 5.6 Hz, dmb-5,5′), 6.80−6.64 (m, 24H, Ph-*o*), 2.32 (s, 12H, -C$\underline{H}_3$), 1.29−1.24 (m, 12H, PPh_2-(C$\underline{H}_2$)$_2$-PPh_2). FT-IR (in MeCN) ν_{CO}/cm^{-1}: 1931, 1878, 1862, 1850. ESI-MS (in MeCN) *m*/*z*: 816 [M − 3PF_6^-]$^{3+}$. Analysis obtained for $C_{118}H_{104}F_{18}N_6O_6P_9Re_3$: C, 49.19; H, 3.64; N, 2.92 (calculated), and C, 48.95; H, 3.64; N, 2.79% (found).

Photochemical Multielectron Accumulation. A DMF−TEOA (5:1 v/v) solution containing the **R4P(*x*)**$^{4+}$ (*x* = 2−6, 0.05 mM) or **R6P(4)**$^{6+}$ (0.033 mM) complexes was degassed by the freeze−pump−thaw method, and then irradiated using 436 nm monochromatic light obtained using a high-pressure mercury lamp (Ushio USH-500SC) combined with a 5 cm long $CuSO_4$ solution filter (250 g L^{-1}), a band-pass filter (Asahi Spectra Co., with a full width at half-maximum of 10 nm), and neutral density (ND) filters (Chuo Precision Industrial Co.). During irradiation, the temperature of the solution was maintained at (25 ± 0.1) °C using an IWAKI constant-temperature system CTS-134A. In situ measurements of UV−vis absorption spectra were conducted using a Photal MCPD-2000 spectrometer or a Photal MCPD-9800 spectrometer. The incident light intensity at 436 nm was determined using a $K_3Fe(C_2O_4)_3$ chemical actinometer.[16]

CONCLUSION

A new synthesis method for ring-shaped trinuclear, tetranuclear, and hexanuclear Re(I) complexes was developed. In an acetone−water mixture, two carbonyl ligands in both edge units of the corresponding liner-shaped trinuclear, tetranuclear, and hexanuclear complexes could be selectively substituted with solvent molecules by photochemical reaction. These solvento complexes reacted with a bidentate phosphorus ligand to afford ring-shaped complexes with much higher yields compared with the previously reported method. This method was successfully applied to synthesis of a ring-shaped trinuclear complex with different types of Re(I) units.

The tetranuclear and hexanuclear complexes could photochemically accumulate 2.9−3.6 and 4.4 electrons in one molecule, respectively. These reduced complexes were relatively stable in solution, where all individual reduced Re(I) units had high reduction powers (from −1.66 to −1.76 V vs Ag/$AgNO_3$) because the electrons were stored in the Re(I) units one by one.

ASSOCIATED CONTENT

Supporting Information

Estimation method of the inner filter effect, procedures for syntheses, and supporting figures. This material is available free of charge via the Internet at http://pubs.acs.org.

AUTHOR INFORMATION

Corresponding Author

*E-mail: ishitani@chem.titech.ac.jp.

Notes

The authors declare no competing financial interest.

ACKNOWLEDGMENTS

This work was partially supported by a Grant-in-Aid for Scientific Research on Innovate Areas “Artificial Photosynthesis (AnApple)” (No. 24107005) from the Japan Society for the Promotion of Science (JSPS).

REFERENCES

(1) (a) Ishida, H.; Terada, T.; Tanaka, K.; Tanaka, T. *Inorg. Chem.* **1990**, *29*, 905−911. (b) Lehn, J.-M.; Ziessel, R. *J. Organomet. Chem.* **1990**, *382*, 157−173.

(2) (a) Hawecker, J.; Lehn, J.-M.; Ziessel, R. *Helv. Chim. Acta* **1986**, *69*, 1990−2012. (b) Ishitani, O.; George, M. W.; Ibusuki, T.; Johnson, F. P. A.; Koike, K.; Nozaki, K.; Pac, C.; Turner, J. J.; Westwell, J. R. *Inorg. Chem.* **1994**, *33*, 4712−4717. (c) Hayashi, Y.; Kita, S.; Brunschwig, B. S.; Fujita, E. *J. Am. Chem. Soc.* **2003**, *125*, 11976−11987. (d) Takeda, H.; Koike, K.; Inoue, H.; Ishitani, O. *J. Am. Chem. Soc.* **2008**, *130*, 2023−2031. (e) Roy, S.; Blane, T.; Lilio, A.; Kubiak, C. P. *Inorg. Chim. Acta* **2011**, *374*, 134−139. (f) Andrade, G. A.; Pistner, A. J.; Yap, G. P. A.; Lutterman, D. A.; Rosenthal, J. *ACS Catal.* **2013**, *3*, 1685−1692. (g) Teesdale, J. J.; Pistner, A. J.; Yap, G. P. A.; Ma, Y.-Z.; Lutterman, D. A.; Rosenthal, J. *Catal. Today* **2014**, *225*, 149−157.

(3) Arachchige, S. M.; Brown, J. R.; Chang, E.; Jain, A.; Zigler, D. F.; Rangan, K.; Brewer, K. J. *Inorg. Chem.* **2009**, *48*, 1989−2000.

(4) (a) Goldsmith, J. I.; Hudson, W. R.; Lowry, M. S.; Anderson, T. H.; Bernhard, S. *J. Am. Chem. Soc.* **2005**, *127*, 7502−7510. (b) Gärtner, F.; Cozzula, D.; Losse, S.; Boddien, A.; Anilkumar, G.; Junge, H.; Schulz, T.; Marquet, N.; Spannenberg, A.; Gladiali, S.; Beller, M. *Chem.—Eur. J.* **2011**, *17*, 6998−7006.

(5) (a) Wouters, K. L.; de Tacconi, N. R.; Konduri, R.; Lezna, R. O.; MacDonnell, F. M. *Photosynth. Res.* **2006**, *87*, 41−55. (b) Lezna, R. O.; De Tacconi, N. R.; MacDonnell, F. *ECS Trans.* **2008**, *11*, 37−43. (c) Singh, S.; de Tacconi, N. R.; Boston, D.; MacDonnell, F. M. *Dalton Trans.* **2010**, *39*, 11180−11187. (d) Polyansky, D. E.; Cabelli, D.; Muckerman, J. T.; Fukushima, T.; Tanaka, K.; Fujita, E. *Inorg. Chem.* **2008**, *47*, 3958−3968. (e) Fukushima, T.; Fujita, E.; Muckerman, J. T.; Polyansky, D. E.; Wada, T.; Tanaka, K. *Inorg. Chem.* **2009**, *48*, 11510−11512. (f) Fukushima, T.; Wada, T.; Ohtsu, H.; Tanaka, K. *Dalton Trans.* **2010**, *39*, 11526−11534.

(6) Kitamoto, K.; Sakai, K. *Angew. Chem., Int. Ed.* **2014**, *53*, 4618−4622.

(7) (a) Koike, K.; Tanabe, J.; Toyama, S.; Tsubaki, H.; Sakamoto, K.; Westwell, J. R.; Johnson, F. P. A.; Hori, H.; Saitoh, H.; Ishitani, O. *Inorg. Chem.* **2000**, *39*, 2777−2783. (b) Morimoto, T.; Nishiura, C.; Tanaka, M.; Rohacova, J.; Nakagawa, Y.; Funada, Y.; Koike, K.; Yamamoto, Y.; Shishido, S.; Kojima, T.; Saeki, T.; Ozeki, T.; Ishitani, O. *J. Am. Chem. Soc.* **2013**, *135*, 13266−13269.

(8) (a) Tsubaki, H.; Sekine, A.; Ohashi, Y.; Koike, K.; Takeda, H.; Ishitani, O. *J. Am. Chem. Soc.* **2005**, *127*, 15544−15555. (b) Tsubaki, H.; Tohyama, S.; Koike, K.; Saitoh, H.; Ishitani, O. *Dalton Trans.* **2005**, 385−395. (c) Morimoto, T.; Ito, M.; Koike, K.; Kojima, T.; Ozeki, T.; Ishitani, O. *Eur. J. Chem.* **2012**, *18*, 3292−3304.

(9) Ishitani, O.; Kanai, K.; Yamada, Y.; Sakamoto, K. *Chem. Commun.* **2001**, 1514−1515.

(10) Yamamoto, Y.; Sawa, S.; Funada, Y.; Morimoto, T.; Falkenström, M.; Miyasaka, H.; Shishido, S.; Ozeki, T.; Koike, K.; Ishitani, O. *J. Am. Chem. Soc.* **2008**, *130*, 14659−14674.
(11) When **L4P(4)-(Sol)$_2$**$^{4+}$ reacted with the bidentate phosphorous ligands without exchange of the Sol ligand with MeCN, the isolated yield of **R4P(4)**$^{4+}$ decreased.
(12) Yamamoto, Y.; Tamaki, Y.; Yui, T.; Koike, K.; Ishitani, O. *J. Am. Chem. Soc.* **2010**, *132*, 11743−11752.
(13) Flanagan, J. B.; Margel, S.; Bard, A. J.; Anson, F. C. *J. Am. Chem. Soc.* **1978**, *100*, 4248−4253.
(14) The UV−vis absorption spectrum of the OERS of the Re(I) unit(s) in **R4P(2)**$^{4+}$ (Supporting Information, Figure S8a) was different from those of the other **RnP(*x*)**$^{n+}$ probably because of the stronger $\pi-\pi$ interaction between the bpy ligand and the phenyl groups of the phosphorous ligand owing to smaller inside space of **R4P(2)**$^{4+}$ compared with the other **RnP(*x*)**$^{n+}$. Therefore, the number of accumulated electrons in **R4P(2)**$^{4+}$ could not be estimated.
(15) Takeda, H.; Yamamoto, Y.; Nishiura, C.; Ishitani, O. *Anal. Sci.* **2006**, *22*, 545−549.
(16) Hatchard, C. G.; Parker, C. A. *Proc. R. Soc. London, Ser. A* **1956**, *235*, 518−536.

dx.doi.org/10.1021/ic501196q | *Inorg. Chem.* 2014, 53, 7170−7180